Inorg. Chem. **2005**, *44*, 6386–6392

Dioxo-Molybdenum(VI) and Mono-oxo-Molybdenum(IV) Complexes Supported by New Aliphatic Dithiolene Ligands: New Models with Weakened Mo═O Bond Characters for the Arsenite Oxidase Active Site

Hideki Sugimoto,*,† Makoto Harihara,† Motoo Shiro,‡ Kunihisa Sugimoto,‡ Koji Tanaka,§ Hiroyuki Miyake,† and Hiroshi Tsukube†

Department of Chemistry, Graduate School of Science, Osaka City University, Sumiyoshi-ku, Osaka, 558-8585, Japan, Rigaku Corporation, Akishima, Tokyo, 196-8666, Japan, and Institute for Molecular Science, Higashiyama, Okazaki, 444-8787, Japan.

Received February 15, 2005

The *cis*-dioxo-molybdenum(VI) complexes, $[MoO_2(L^H)_2]^{2-}$ (**1b**), $[MoO_2(L^S)_2]^{2-}$ (**2b**), and $[MoO_2(L^O)_2]^{2-}$ (**3b**) (L^H = cyclohexene-1,2-dithiolate, L^S = 2,3-dihydro-2H-thiopyran-4,5-dithiolate, and L^O = 2,3-dihydro-2H-pyran-4,5-dithiolate), with new aliphatic dithiolene ligands were prepared and investigated by infrared (IR) and UV–vis spectroscopic and electrochemical methods. The mono-oxo-molybdenum(IV) complexes, $[MoO(L^H)_2]^{2-}$ (**1a**), $[MoO(L^S)_2]^{2-}$ (**2a**), and $[MoO(L^O)_2]^{2-}$ (**3a**), were further characterized by X-ray crystal structural determinations. The IR and resonance Raman spectroscopic studies suggested that these *cis*-dioxo molybdenum(VI) complexes (**1b**–**3b**) had weaker Mo═O bonds than the common $Mo^{VI}O_2$ complexes. Complexes **1b**–**3b** also exhibited strong absorption bands in the visible regions assigned as charge-transfer bands from the dithiolene ligands to the *cis*-MoO_2 cores. Because the oxygen atoms of the *cis*-$Mo^{VI}O_2$ cores are relatively nucleophilic, these complexes were unstable in protic solvents and protonation might occur to produce $Mo^{VI}O(OH)$, as observed with the oxidized state of arsenite oxidase.

Introduction

The crystallographic and EXAFS characterizations of several molybdenum-containing oxotransferase and hydroxylase enzymes have spurred coordination chemists to give much attention to the intriguing coordination structures around their molybdenum centers.[1,2] In the DMSO reductase family that contains molybdenum centers coordinated with two pyranopterin-1,2-dithiolate ligands, the arsenite oxidases have unique molybdenum centers that are not coordinated with amino acid residues.[3,4] Electrochemical studies of the arsenite oxidase have strengthened the significance of the *cis*-dioxo-molybdenum(VI) ($Mo^{VI}O_2$) and mono-oxo-molybdenum(IV) ($Mo^{IV}O$) cores in the oxidized and reduced states.[3] The EXAFS studies suggested that the $Mo^{VI}O_2$ core of arsenite oxidase had one longer Mo^{VI}═O bond at 1.83 Å and that its protonated, $Mo^{VI}O(OH)$, form may be involved in the catalytic cycle.[4,5] Although X-ray crystallographic studies on the oxidized state of arsenite oxidase indicated that the $Mo^{IV}O$ species forms from an auto-photoreduction of the Mo(VI) state,[4] the $Mo^{VI}O_2$ core is considered to have relatively weak Mo═O bonds and basic oxygen atoms.

A number of $Mo^{VI}O_2$ complexes have been presented as structural and functional models of molybdenum active sites.[2b,6] Most of them were neutral complexes that contained

* To whom correspondence should be addressed. E-mail: sugimoto@sci.osaka-cu.ac.jp.
† Osaka City University.
‡ Rigaku Corporation.
§ Institute for Molecular Science.

(1) (a) Messerschmidt, A.; Huber, R.; Poulos, T.; Wieghardt, K. *Handbook of Metalloproteins*; John Wiley & Sons: New York, 2000; p 1024. (b) Burgmayer, S. J. N. In *Progress in Inorganic Chemistry*; Karlin, K. D., Stiefel, E. I., Eds.; John Wiley & Sons: New York, 2003; Vol. 52; p 491.
(2) (a) Hille, R. *Chem. Rev.* **1996**, *96*, 2757. (b) McMaster, J.; Tunney, J. M.; Garner, C. D. In *Progress in Inorganic* Chemistry; Karlin, K. D., Stiefel, E. I., Eds.; John Wiley & Sons: New York, 2004; Vol. 52, p 539.
(3) Hoke, K. R.; Cobb, N.; Armstrong, F. A.; Hille, R. *Biochemistry* **2004**, *43*, 1667.
(4) Ellis, P. J.; Conrads, T.; Hille, R.; Kuhn, P. *Structure* **2001**, *9*, 125.
(5) Conrads, T.; Hemann, C.; George, G. N.; Pickering, I. J.; Prince, R. C.; Hill, R. *J. Am. Chem. Soc.* **2002**, *124*, 11276.
(6) (a) Holm, R. H. *Chem. Rev.* **1987**, *87*, 1401. (b) Holm, R. H. *Coord. Chem. Rev.* **1990**, *100*, 183. (c) Enemark, J. H.; Young, C. G. *Adv. Inorg. Chem.* **1994**, *40*, 1. (d) Enemark, J. H.; Cooney, J. J. A.; Wang, J.-J.; Holm. R. H. *Chem. Rev.* **2004**, *104*, 1175.

10.1021/ic050234p CCC: $30.25
Published on Web 08/02/2005

Chart 1. Designations of Complex Structures and Abbreviations

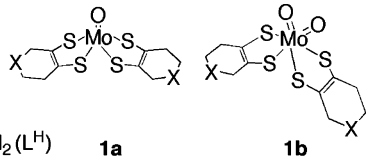

X = CH_2 (L^H)	**1a**	**1b**
= S (L^S)	**2a**	**2b**
= O (L^O)	**3a**	**3b**

weaker electron-donating ligands such as dimethyldithiocarbamate (S_2CNMe_2), 2,6-bis(2,2-diphenyl-2-mercaptoethanyl)-pyridine (dmp), and *N*,*N*′-dimethyl−*N*,*N*′-bis(2-mercaptophenyl)ethylenediamine (Sphe).[7−9] Since these $Mo^{VI}O_2$ complexes had short Mo^{VI}═O bond distances, reflecting the strong Lewis acidities of the molybdenum centers and the weak basicities of the oxo groups,[6a−6c] the Mo^{VI}═O bonds were essentially strong and protonation to the $Mo^{VI}O_2$ cores rarely occurred. A few $Mo^{VI}O_2$ bis(dithiolene) complexes, such as $[MoO_2(mnt)_2]^{2-}$ (mnt = 1,2-dicyano-1,2-ethylenedithiolate),[10a] $[MoO_2(bdt)_2]^{2-}$ (bdt = benzene-1,2-dithiolate), and $[MoO_2(bdtR)_2]^{2-}$ (bdtR = alkyl substituted derivatives of bdt),[11] have been reported so far as more suitable structural and functional models for the DMSO reductase family and sulfite oxidase.[2,6] In particular, these types of complexes are expected to give insights into the nature of the molybdenum center in the oxidized state of arsenite oxidase because their structures closely mimic the molybdenum center of the active site, as reported in the electrochemical and EXAFS studies,[3,5] and the complexes are able to mediate oxygen atom transfer reactions without undergoing the competing comproportionation reaction to form undesired dinuclear complexes with the $Mo^{V}_2O_3$ cores.[10] Because the mnt ligand includes strong electron-withdrawing CN groups and the benzene-1,2-dithiolate ligands are aromatic dithiolene ligands,[10a,11] we introduce several aliphatic dithiolene ligands into the $Mo^{VI}O_2$ complexes and characterize them as a new class of model complexes. We have prepared a new series of $Mo^{VI}O_2$ complexes (**1b**−**3b**) supported by cyclohexene-1,2-dithiolate (L^H), 2,3-dihydro-2H-thiopyran-4,5-dithiolate (L^S), and 2,3-dihydro-2H-pyran-4,5-dithiolate (L^O) (Chart 1). The dithiolene ligands employed here have six-membered rings similar to those of the biological pyranodithiolene ligands, and their complexes have the relatively weak Mo═O bonds proposed for the active center in the oxidized state of arsenite oxidase. Although autoredox reactions between the $Mo^{VI}O_2$ cores and the aliphatic dithiolene ligands often occurred in the related $[MoO_2(S_2C_2(CO_2Me)_2)]^{2-}$ and $[MoO_2(S_2C_2Me_2)_2]^{2-}$ systems,[6d] we anticipate that this new series of complexes will act as more suitable models with weakened Mo═O bond characteristics for the active center.

Experimental Section

General. All reagents and solvents were used as received unless otherwise noted. Acetonitrile was dried over CaH_2 and then P_2O_5 and was distilled under argon prior to use. All reactions were carried out under argon in a Schlenk tube or a Miwa DB0-1KP glovebox. $C_6H_8S_2CO$ (L^HCO) was prepared by following the literature.[12]

Synthesis and Characterization of Complexes. C_5SH_7OBr. Br_2 (0.8 mL, 15.4 mmol) was added to a suspension of CCl_4 (200 mL) containing tetrahydro-4*H*-thiopyran-4-one (2.0 g, 17 mmol) and K_2CO_3 (2.4 g, 17.5 mmol). After the mixture was filtered, the pale yellow filtrate was concentrated to dryness. After it was extracted with $CHCl_3/H_2O$, a colorless oil of C_5SH_7OBr was obtained. The C_5SH_7OBr obtained was very unstable and was used without characterization. EI-MS: *m*/*z* 197 $[C_5H_7OSBr]^+$.

$C_5SH_7OS_2CO^iPr$. Solid potassium isopropylxanthate (2.5 g, 14 mmol) was added to the C_5SH_7OBr in acetone (30 mL). The solution was stirred for 30 min at 60 °C and concentrated to remove the acetone. HCl (10%) was added to the yellow solid in H_2O (20 mL) to adjust the solution pH to 3−4. After the solution was stirred for 10 min, extraction with ether and concentration gave a yellow solid of $C_5SH_7OS_2CO^iPr$. Yield: 2.5 g (60%). ^1H NMR ($CDCl_3$): δ 1.39 (dd, 6H), 2.84−3.15 (m, 5H), 3.39 (dquin, 1H), 4.83 (dquin, 1H), 5.72 (h, 1H).

$C_5SH_6S_2CO$ (L^SCO). $HClO_4$ (70%, 3 mL) was added to solid $C_5SH_7OS_2CO^iPr$ (1.0 g, 4 mmol) at 0 °C. The addition of ice to the red solution yielded a white solid. The solid was collected by filtration, washed with H_2O, and dried in vacuo. Yield: 0.3 g (40%). EI-MS: *m*/*z* 190 $[C_6H_6S_3O]^+$. ^1H NMR ($CDCl_3$): δ 2.75 (m, 2H), 2.97 (t, 2H), 3.46 (t, 2H).

C_5OH_7OBr. This compound was prepared as described above for C_5SH_7OBr, but tetrahydro-4*H*-pyran-4-one was used instead of tetrahydro-4*H*-thiopyran-4-one. EI-MS: *m*/*z* 179 $\{C_5H_7O_2Br\}^+$. ^1H NMR ($CDCl_3$): δ 2.66 (m, 1H), 3.00 (m, 1H), 3.94 (m, 2H), 4.10 (quin, 1H), 4.29 (quin, 1H), 4.48 (quin, 1H).

$C_5OH_7OS_2CO^iPr$. This compound was prepared as described above for $C_5SH_7OS_2CO^iPr$, but C_5OH_7OBr was used instead of C_5SH_7OBr. EI-MS: *m*/*z* 233 $[C_9H_{14}O_3S_2]^+$. ^1H NMR ($CDCl_3$): δ 1.39 (dd, 6H), 2.66 (dt, 1H), 2.81 (m, 1H), 3.68 (t, 1H), 3.82 (dt, 1H), 4.27 (m, 1H), 4.43 (quin, 1H), 4.68 (quin, 1H), 5.73 (h, 1H).

$C_5OH_6S_2CO$ (L^OCO). H_2SO_4 (98%, 4 mL) was added to solid $C_5OH_7OS_2CO^iPr$ (5.0 g, 21 mmol) at 0 °C. The addition of ice to the suspension yielded a pale gray solid. The solid was collected by filteration, washed with 2-propanol, and dried in vacuo. Yield: 3.0 g (80%). EI-MS: *m*/*z* 174 $[C_6H_6S_2O_2]^+$. The compound did not have enough solubility to measure the ^1H NMR spectrum.

$[Ni(L^H)_2]$. NaOH (0.23 g, 5.7 mmol) in methanol (20 mL) was added to a methanol suspension (30 mL) of L^HCO (0.5 g, 2.9 mmol). Within 30 min, the suspension of L^HCO changed to a yellow solution, and $NiCl_2{\cdot}6H_2O$ (0.34 g, 1.4 mmol) in CH_3OH (30 mL) was added. $(NH_4)_2Ce(NO_3)_6$ (1.5 g, 2.7 mmol) in CH_3OH (30 mL) was added to the resultant red-purple solution, until the red-purple solution changed to blue. The blue precipitated powder was collected by filtration and dissolved in CH_2Cl_2 (200 mL). After filtration to remove any undissolved solids, the blue solution was concentrated to yield a blue powder. Yield: 0.35 g (60%). Anal. Calcd for $C_{12}H_{16}NiS_4$ (mol wt 347.2): C, 27.54; H, 3.08. Found: C, 27.63; H, 2.95. UV−vis spectrum (CH_2Cl_2): 309 (20000), 438 (1600), 591 (1500), 787 nm (15000 $dm^3mol^{-1}cm^{-1}$). IR (KBr): ν 970 (vs), 1325 (s), 1340 (s), 1367 (vs), 1419 cm^{-1} (s).

$[Ni(L^S)_2]$. This complex was prepared as described above for $[Ni(L^H)_2]$, but L^SCO was used instead of L^HCO. Yield: 70%. Anal.

(7) Moore, F. W.; Larson, M. L. *Inorg. Chem*. **1967**, *6*, 998.
(8) Dowerah, D.; Spence, J. T.; Singh, R.; Wedd, A. G.; Wilson, G. L.; Farchione, F.; Enemark, J. H.; Kristofzski, J.; Bruck, M. *J. Am. Chem. Soc*. **1987**, *109*, 5655.
(9) Berg, J. M.; Holm, R. H. *J. Am. Chem. Soc*. **1985**, *107*, 917.
(10) (a) Das, S. K.; Chaudhury, P. K.; Biswas, D.; Sarker, S. *J. Am. Chem. Soc*. **1994**, *116*, 9061. (b) Tucci, G. C.; Donahue, J. P.; Holm. R. H. *Inorg. Chem*. **1998**, *37*, 1602. (c) Lober, C.; Plutino, M. R.; Elding, L. I.; Nordlander, E. *J. Chem. Soc., Dalton Trans*. **1997**, 3997.
(11) Ueyama, N.; Oku, H.; Kondo, M.; Okamura, T.; Yoshinaga, N.; Nakamura, A. *Inorg. Chem*. **1996**, *35*, 643.
(12) Bhattacharya, A. K.; Hortmann, A. G. *J. Org. Chem*. **1974**, *39*, 95.

Calcd for $C_{10}H_{12}NiS_6 \cdot 0.3H_2O$ (mol wt 388.7): C, 30.90; H, 3.28. Found: C, 30.83; H, 3.28. UV−vis spectrum (CH_2Cl_2): 310 (17000), 602 (1000), 785 nm (10000 $dm^3mol^{-1}cm^{-1}$). IR (KBr): ν 926 (s), 976 (m), 1370 (vs), 1417 cm^{-1} (s).

[Ni(L^O)$_2$]. This complex was prepared as described above for [Ni(L^H)$_2$], but L^{O}CO was used instead of L^{H}CO. Yield: 70%. Anal. Calcd for $C_{10}H_{12}NiO_2S_4$ (mol wt 351.2): C, 34.20; H, 3.44. Found: C, 34.03; H, 3.31. UV−vis spectrum (CH_2Cl_2): 306 (26000), 430 (1800, sh), 582 (2000), 778 nm (18000 $dm^3mol^{-1}cm^{-1}$). IR (KBr): ν 966 (s), 996 (vs), 1097 (m), 1385 (vs), 1420 cm^{-1} (vs).

[Mo(CO)$_2$(L^H)$_2$]. This complex was prepared as described in the literature.[13] A CH_2Cl_2 (100 mL) suspension containing [Ni(L^H)$_2$] (0.5 g, 1.5 mmol) and [Mo(CO)$_3$(CH$_3$CN)$_3$] (0.25 g, 0.8 mmol) was stirred for 3 days, and the blue suspension changed to a red-purple. After filtration, the filtrate was concentrated to dryness. Purification by silica gel column chromatography (Wakogel C-200; eluent, hexane/chloroform = 9/1) gave a red-purple microcrystalline powder, which was collected by filtration and dried in air. Yield: 80 mg (20%). Anal. Calcd for $C_{14}H_{16}MoO_2S_4$ (mol wt 512.6): C, 38.17; H, 3.66. Found: C, 38.23; H, 3.54. UV−vis spectrum (CH_2Cl_2): 304 (5000), 400 (8000), 538 nm (15000 $dm^3mol^{-1}cm^{-1}$). IR (KBr): ν 1472 (s), 1979 (vs), 2023 cm^{-1} (vs).

[Mo(CO)$_2$(L^S)$_2$]. This complex was prepared as described above for [Mo(CO)$_2$(L^H)$_2$] but [Ni(L^S)$_2$] was used instead of [Ni(L^H)$_2$]. Yield: 10%. Anal. Calcd for $C_{12}H_{12}MoO_2S_6$ (mol wt 476.6): C, 30.24; H, 2.54. Found: C, 30.16; H, 2.61. UV−vis spectrum (CH_2Cl_2): 304 (5000), 400 (8000), 538 nm (15000 $dm^3mol^{-1}cm^{-1}$). IR (KBr): ν 1479 (m), 1989 (s), 2033 cm^{-1} (vs).

[Mo(CO)$_2$(L^O)$_2$]. This complex was prepared as described above for [Mo(CO)$_2$(L^H)$_2$], but [Ni(L^O)$_2$] was used instead of [Ni(L^H)$_2$]. Yield: 20%. Anal. Calcd for $C_{12}H_{12}MoO_4S_4$ (mol wt 444.4): C, 38.90; H, 3.87. Found: C, 38.92; H, 3.67. UV−vis spectrum (CH_2Cl_2): 304 (4500), 400 (7000), 536 nm (13000 $dm^3mol^{-1}cm^{-1}$). IR (KBr): ν 1486 (s), 1989 (s), 2031 cm^{-1} (vs).

(Et$_4$N)$_2$[MoO(L^H)$_2$] (1a). Et$_4$NOH/methanol (230 μL, 25%) was added to a THF solution containing [Mo(CO)$_2$(L^H)$_2$] (90 mg, 0.18 mmol). After the mixture was stirred for 12 h, a yellow-green powder precipitated out of the solution and was collected by filtration. Orange crystals of **1a** were recrystallized from acetonitrile/ether. Yield: 70 mg (60%). Anal. Calcd for $C_{28}H_{56}MoN_2OS_4$ (mol wt 661.0): C, 49.53; H, 8.61; N, 4.13. Found: C, 49.31; H, 8.42; N, 3.99. UV−vis spectrum (CH$_3$CN): 260 (18000), 310 (7000), 476 nm (300 $dm^3\ mol^{-1}\ cm^{-1}$). IR (KBr): ν 896 (vs), 1004 (m), 1172 (m), 1480 cm^{-1} (vs).

(Et$_4$N)$_2$[MoO(L^S)$_2$] (2a). This complex was prepared as described above for **1a**, but [Mo(CO)$_2$(L^S)$_2$] was used instead of [Mo(CO)$_2$(L^H)$_2$]. Yield: 50%. Anal. Calcd for $C_{28}H_{52}MoN_2OS_6$ (mol wt 697.0): C, 44.80; H, 7.52; N, 4.02. Found: C, 44.70; H, 7.74; N, 4.11. UV−vis spectrum (CH$_3$CN): 260 (18000), 310 (7000), 476 nm (300 $dm^3\ mol^{-1}\ cm^{-1}$). IR (KBr): ν 899 (vs), 1002 (m), 1172 (m), 1479 cm^{-1} (vs).

(Et$_4$N)$_2$[MoO(L^O)$_2$] (3a). This complex was prepared as described above for **1a**, but [Mo(CO)$_2$(L^O)$_2$] was used instead of [Mo(CO)$_2$(L^H)$_2$]. Yield: 60%. Anal. Calcd for $C_{28}H_{52}MoN_2O_3S_4$ (mol wt 664.9): C, 46.97; H, 7.88; N, 4.21. Found: C, 46.72; H, 7.93; N, 4.02. UV−vis spectrum (CH$_3$CN): 260 (27000), 307 (12000), 476 nm (400 $dm^3\ mol^{-1}\ cm^{-1}$). IR (KBr): ν 902 (vs), 1091 (m), 1172 (m), 1480 cm^{-1} (vs).

Physical Measurements. FT-IR spectra were recorded with a Perkin-Elmer Spectrum One spectrometer. Resonance Raman spectra were taken on a Jasco NRS-1000 instrument using an Ar^+ ion laser with excitation at 610 nm. UV−vis spectra were recorded on Shimazu UV-2550, HP-8452, and UNISOKU USP-801 spectrometers. ^{1}H NMR spectra were measured on a JEOL-Lambda 300 (300 MHz) spectrometer.

Table 1. Crystallographic Informations for (Ph$_4$P)$_2$[MoO(L^H)$_2$] (**1a**), (Et$_4$N)$_2$[MoO(L^S)$_2$] (**2a**), and (Et$_4$N)$_2$[MoO(L^O)$_2$] (**3a**)

	1a	2a	3a
formula	$C_{60}H_{56}MoOP_2S_4$	$C_{26}H_{52}N_2MoOS_6$	$C_{26}H_{52}N_2MoO_3S_4$
fw	1079.23	697.02	664.89
size (mm)	0.25 × 0.20 × 0.03	0.30 × 0.20 × 0.15	0.30 × 0.15 × 0.10
temp(K)	93.2	123.1	123.1
cryst syst	monoclinic	orthorhombic	orthorhombic
space group	$P2_1$ (No. 4)	*Pnma* (No. 62)	*Pnma* (No. 62)
Z	2	4	4
a (Å)	10.9428(8)	18.483(7)	18.359(2)
b (Å)	15.0291(7)	11.457(5)	11.436(2)
c (Å)	15.14217(12)	15.721(6)	15.226(3)
α (deg)	90	90	90
β (deg)	92.503(1)	90	90
γ (deg)	90	90	90
V (Å^3)	2487.8(3)	3329.0(23)	3196.8(10)
μ (mm^{-1})	0.539	0.663	0.699
GOF	1.272	0.974	1.096
R_1 (R_2)	6.28 (15.06)	9.50 (29.30)	9.70 (25.90)

Electrochemistry. Cyclic voltammetric measurements were performed under nitrogen with a Hokuto Denko HZ-3000 potentiostat. A three-electrode configuration consisting of a glassy-carbon working electrode, a SCE reference electrode, and a platinum counter electrode was used.

X-ray Crystallography. A single crystal of (Ph$_4$P)$_2$[MoO(L^H)$_2$] was obtained by adding Ph$_4$PBr to an acetonitrile solution of (Et$_4$N)$_2$[MoO(L^H)$_2$] and was mounted on a glass fiber with traces of viscous oil. The X-ray data were collected with graphite-monochromated Mo Kα radiation on a Rigaku/MSC Mercury CCD diffractometer at −150 °C. The structures were solved by direct methods (SIR-97)[14] and expanded using DIRDIF 99.[15] The atoms were refined anisotropically, except for the disordered atoms, by full-matrix least squares on F^2. The non-hydrogen atoms in all structures were attached at idealized positions on carbon atoms, except for disordered atoms, and were not refined. All structures converted in the final stages of refinement showed no movement in the atom positions. Calculations for **1a** were performed using TEXSAN.[16] Calculations for **2a** and **3a** were performed using Single-Crystal Structure Analysis Software, version 3.5.1.[17] The crystallographic parameters of (Ph$_4$P)$_2$[MoO(L^H)$_2$] (**1a**), (Et$_4$N)$_2$[MoO(L^S)$_2$] (**2a**), and (Et$_4$N)$_2$[MoO(L^O)$_2$] (**3a**) are summarized in Table 1.

Results and Discussion

Mo^{IV}O Complexes. As [Mo^{VI}O$_2$(mnt)$_2$]$^{2-}$ and [Mo^{VI}O$_2$(benzene-1,2-dithiolate)$_2$]$^{2-}$ were obtained from the reaction of the corresponding Mo^{IV}O complexes with Me$_3$NO,[11] we synthesized the Mo^{IV}O complexes, **1a**− **3a**, with new

(13) Lim, B. S.; Donahue, J. P.; Holm, R. H. *Inorg. Chem*. **2000**, *39*, 263.

(14) Altomare, A.; Burla, M.; Camalli, M.; Cascarano, G.; Giacovazzo, C.; Guagliardi, A.; Moliterni, A.; Polidori, G.; Spagna, R. *J. Appl. Cryst*. **1999**, *32*, 115.

(15) Beurskens, P. T.; Admiraal, G.; Beurskens, G.; Bosman, W. P.; de Gelder, R.; Israel, R.; Smits, J. M. M. *The DIRDIF-99 Program System*; Technical Report of the Crystallography Laboratory; University of Nijmegen: The Netherlands, 1999.

(16) Rigaku/MSC, 9009 New Trails Drive, The Woodlands, TX, USA 77381. Rigaku, 3-9-12 Akishima, Tokyo 196-8666, Japan.

(17) *Single-Crystal Structure Analysis Package*; Molecular Structure Corporation: Woodlands, TX, 1992.

Scheme 1. Preparation of $[MoO(L^X)_2]^{2-}$ and $MoO_2(L^X)_2]^{2-}$

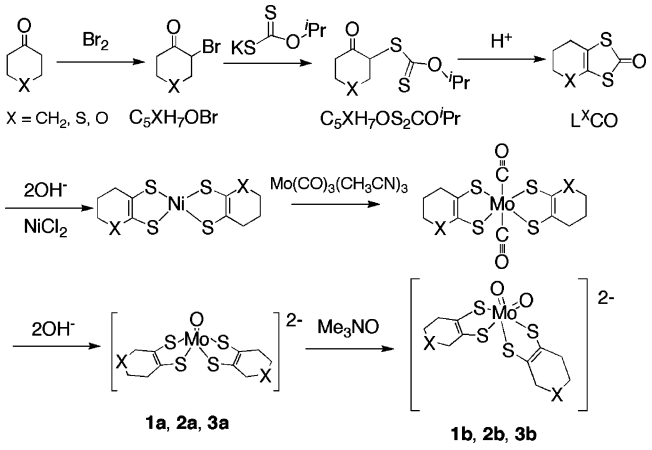

aliphatic dithiolene ligands L^H, L^S, and L^O as precursors of the $Mo^{VI}O_2$ complexes. We referred to the literature by C. Garner et al. and R. Holm et al., in which strategies for the synthesis of various types of $Mo^{IV}O$ bis(dithiolene) complexes were given, to synthesize **1a**−**3a** (Scheme 1).[13,21] The ligand precursors L^XCO (X = H, S, and O) were hydrolyzed with 2 equiv of NaOH to give the dianionic species L^{X2-}. After the reaction of $2L^{X2-}$ with $NiCl_2 \cdot 6H_2O$, the oxidation of the $[Ni(L^X)_2]^{2-}$ formed by reaction with Ce(IV) produced neutral $[Ni(L^X)_2]$. The transfer of L^X from the nickel complex to the molybdenum center of $[Mo(CO)_3(CH_3CN)_3]$ yielded $[Mo(CO)_2(L^X)_2]$, and the resulting complexes were readily hydrolyzed by 2 equiv of Et_4NOH to produce **1a**−**3a**.

Figure 1 shows the crystal structure of the anion part of **1a**. The molybdenum(IV) center was coordinated with an oxo group and four sulfur atoms from the two dithiolene ligands, and it adopted a square-pyramidal structure. The molybdenum centers of complexes **2a** and **3a** were also confirmed to have similar square-pyramidal structures (Figure S1). The averaged Mo−S distances at 2.40, 2.37, and 2.39 Å for **1a**−**3a**, respectively, are similar to that of the reduced state of arsenite oxidase (2.37 Å).[4,5] The molybdenum atoms were raised above the basal plane (S1−S4) by 0.70 (**1a**), 0.76 (**2a**), and 0.75 Å (**3a**). The reduced form of arsenite oxidase adopted a similar distorted square-pyramidal structure to that seen in **1a**−**3a** (0.8 Å = the distance from Mo to the basal plane),[4] indicating that compounds **1a**−**3a** may serve as effective structural models. Table 2 lists values of the Mo═O bond lengths, ν(Mo═O) bands, and redox potentials of complexes **1a**−**3a**, together with those of related $Mo^{IV}O$ complexes from the literature. In terms of standard deviations, the Mo═O distances (1.745(6) Å for **1a**, 1.707(8) Å for **2a**, and 1.699(6) Å for **3a**) are not significantly different from one another and are similar to those of the $Mo^{IV}O$ complexes with the mnt, $S_2C_2(CO_2Me)_2$, and bdt ligands (1.67(1), 1.686(6), and 1.699(6) Å).[18−20] In contrast, an IR study revealed that complexes **1a**−**3a** have significantly lower ν(Mo═O) values (896 cm^{-1} for **1a**, 899 cm^{-1} for **2a**, and 902 cm^{-1} for **3a**) than those of the above $Mo^{IV}O$ complexes (932 cm^{-1} for the mnt complex, 914 cm^{-1} for the $S_2C_2(CO_2Me)_2$ complex, and 905 cm^{-1} for the bdt complex).[18−20] These IR results indicate that the new complexes have weak Mo═O bonds and that their molybdenum centers are weak Lewis acids.

As shown in Figures 2 and S2, complexes **1a**−**3a** showed two reversible $[MoO]^{-/2-}$ and $[MoO]^{0/-}$ waves, although the $Mo^{IV}O$ complexes, including the $S_2C_2(CO_2Me)_2$,[19] bdt derivatives,[20,22] sdt (1-phenyl-1,2-ene-dithiolate),[21] edt (1,2-

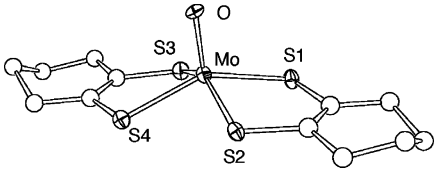

Figure 1. Crystal structure of the anion part of $(Ph_4P)_2[MoO(L^H)_2]$ (**1a**) shown with 50% ellipsoids. The hydrogen atoms were omitted for clarity.

Table 2. Selected Properties of $Mo^{IV}O$ Complexes

	ν(Mo═O) (cm^{-1})	Mo═O (Å)	$E_{1/2}$ V vs SCE $[Mo]^{-/2-}$	$E_{1/2}$ V vs SCE $[Mo]^{0/-}$	ref
$(Et_4N)_2[MoO(L^H)_2]$ (**1a**)	896	1.745(6)	−0.70	+0.06	*a*
$(Et_4N)_2$ $[MoO(L^S)_2]$ (**2a**)	899	1.707(8)	−0.57	+0.18	*a*
$(Et_4N)_2$ $[MoO(L^O)_2]$ (**3a**)	902	1.699(6)	−0.56	+0.19	*a*
$(Et_4N)_2[MoO(mnt)_2]$	932	1.67(1)	+0.48		18
$(Et_4N)_2[MoO(S_2C_2(CO_2Me)_2)_2]$[c]	914	1.686(6)	−0.03		19
$(Et_4N)_2[MoO(bdt)_2]$	905	1.699(6)	−0.35[b]		20
$(Et_4N)_2[MoO(S_2C_2Me_2)_2]$[d]	889	1.712(2)	−0.62	+0.15	13
$(Ph_4P)_2[MoO(sdt)_2]$[e]	879	1.700(5)	−0.48[b]		21

[a] This work. [b] In DMF. [c] $S_2C_2(CO_2Me)_2$ = dicarboxylmethyl-1,2-ethylenedithiolate. [d] $S_2C_2Me_2$ = dimethyl-1,2-ethylenedithiolate. [e] sdt = 1-phenyl-1,2-ene-dithiolate.

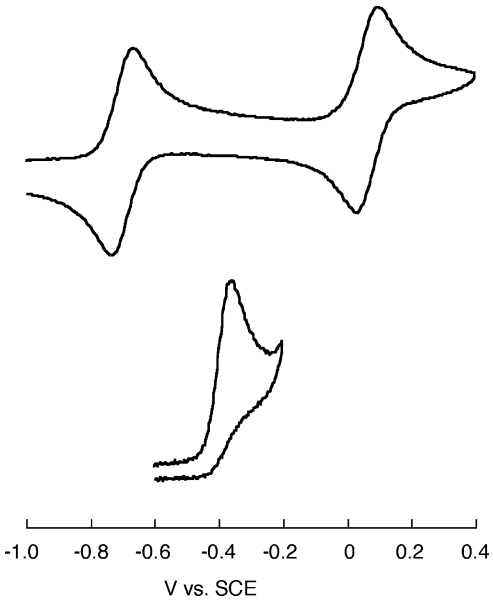

Figure 2. Cyclic voltammograms of $[MoO(L^H)_2]^{2-}$ (**1a**, above) and $[MoO_2(L^H)_2]^{2-}$ (**1b**, below): 1.0 mM of complexes in CH_3CN containing 0.1 M $TBAPF_6$; scan rate = 0.1 V s^{-1}.

(18) Donahue, J. P.; Goldsmith, C. R.; Nadiminti, U.; Holm, R. H. *J. Am. Chem. Soc*. **1998**, *120*, 12869.
(19) Coucouvanis, D.; Hadjikyriacou, A.; Toupadakis, A.; Koo, S.-M.; Draganjac, M. *Inorg. Chem*. **1991**, *30*, 754.
(20) Boyde, S.; Ellis, S. R.; Garner, C. D.; Clegg, W. *J. Chem. Soc., Chem. Comm*. **1986**, 1541.
(21) Davis, E. S.; Beddoes, R. L.; Collison, D.; Dinsmore, A.; Docrat, A.; Joule, J. A.; Wilson, C. R.; Garner, C. D. *J. Chem. Soc., Dalton Trans*. **1997**, 3985.
(22) Oku, H.; Ueyama, N.; Kondo, M.; Nakamura, A. *Inorg. Chem*. **1994**, *33*, 209.

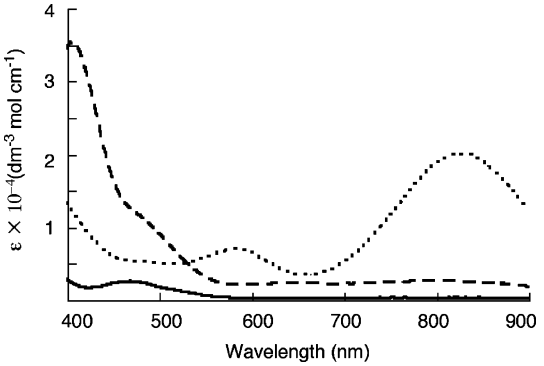

Figure 3. Electronic spectra of 0.2 mM solutions of $[Mo^{IV}O(L^H)_2]^{2-}$ (solid line), $[Mo^{V}O(L^H)_2]^{-}$ (dotted line), and $[Mo^{VI}O(L^H)_2]^{0}$ (dashed line) in CH_3CN.

ethylenedithiolate),[23] and mnt ligands,[18] were reported to give reversible $[MoO]^{-/2-}$ waves and either irreversible or no $[MoO]^{0/-}$ waves.[18−23] Table 2 also shows that complexes **1a**−**3a** generally exhibit more negative potentials compared to those of most of the $Mo^{IV}O$ complexes listed. Because the L^H, L^S, and L^O ligands employed here were confirmed to have strong electron-donating natures to the molybdenum centers (S(dithiolene) → Mo^{IV}) compared with most of the listed ligands, it is suggested that the strong electron donations decreased the O → Mo^{IV} electron donations to weaken the Mo^{IV}═O bonds and stabilize the high valent $[MoO]^0$ states. The reversible $[MoO]^{0/-}$ redox couple allowed the observation of $[Mo^{VI}O]^0$ states for the first time (Figure 3). Both of the oxidation reactions of **1a**, by a controlled potentiometric technique at +0.3 V and with 1 equiv of the ferrocenium cation, yielded orange $[Mo^{VI}O(L^H)_2]^0$ (Figure 3), which was reduced by a controlled potentiometric technique at −1.0 V to regenerate **1a**. The five-coordinate distorted square-pyramidal $[Mo^{VI}O(L^H)_2]^0$ species did not have a strong absorption band in the visible region. In contrast, the six-coordinate $Mo^{VI}O_2$ and $Mo^{VI}O$ bis(dithiolenes) complexes, such as $[MoO_2(mnt)_2]^{2-}$,[18] $[MoO_2(bdt)_2]^{2-}$,[11] and $[MoO(OPh)(S_2C_2Me_2)_2]^{-}$,[24] had strong absorption bands in the visible region resulting from charge transfers from the dithiolene ligands to the molybdenum(VI) centers.

$Mo^{VI}O_2$ Complexes. The reaction of complexes **1a**−**3a** with Me_3NO yielded the corresponding $Mo^{VI}O_2$ complexes, **1b**−**3b**. Figure 4 illustrates the UV−vis spectral changes induced by the reaction of **1a** with Me_3NO in CH_3CN. The yellow-orange solution of **1a** exhibited a small absorption band centered at 470 nm (ϵ = 300 dm^3 mol^{-1} cm^{-1}) that was tentatively assigned to the d−d transition band on the basis of its intensity. After the reaction of **1a** with Me_3NO, two strong broad absorption bands appeared at 490 nm (ϵ = 4000 dm^3 mol^{-1} cm^{-1}) and 610 nm (ϵ = 3500 dm^3 mol^{-1} cm^{-1}), and a deep-gray reaction solution was obtained. Its ESI-MS exhibited a peak at m/z = 418, indicating the formation of $[Mo^{VI}O_2(L^H)_2]^{2-}$ (**1b**), while the peak for **1a** at m/z = 402 completely disappeared (Figure S3).[25] When the reaction was monitored by IR (Figure 5), the $\nu(Mo^{IV}═O)$ stretching band of **1a** at 896 cm^{-1} gradually decreased in intensity and two new bands gradually appeared at 847 and 813 cm^{-1}; the pattern of the two strong bands was characteristic of the *cis*-dioxo-$Mo^{VI}O_2$ complexes.[8,26] These spectroscopic observations demonstrate that the reaction of **1a** with Me_3NO in CH_3CN produced the $Mo^{VI}O_2$ complex **1b**. The **2b** and **3b** complexes were similarly obtained and characterized by UV−vis, ESI-MS, and IR spectroscopic methods (Figures S3, S4, and S5). On the basis of the intensities, the strong broad absorptions around 490 and 600 nm of **1b**−**3b** are tentatively assigned to charge-transfer bands from the dithiolene S(pπ) orbitals to the Mo(dπ) orbitals in the $Mo^{VI}O_2$ center. Although we could not determine the crystal structures of **1b**−**3b**, they were assumed to have distorted octahedral structures, as reported for $[MoO_2(mnt)_2]^{2-}$ and $[MoO_2(bdt)_2]^{2-}$.[10a,11] As the distorted square-pyramidal mono-oxo-Mo(VI) species, $[Mo^{VI}O(L^H)_2]^0$, (Figure 3) did not exhibit a strong band in the visible region, the coordination numbers and O═Mo−S (dithiolenes) angles must be important factors that permit the appearance of the strong absorption bands for **1b**−**3b** in the visible region. By comparing the $Mo^{IV}O$ complexes with the $Mo^{VI}O_2$ complexes, we found that the redox potentials shifted from −0.70 (**1a**, $E_{1/2}$) for $[MoO]^{-/2-}$ to −0.36 V (**1b**, irreversible, E_{pa}) for $[MoO_2]^{-/2-}$, from −0.57 (**2a**) to −0.27 V (**2b**), and from −0.56 (**3a**) to −0.23 V (**3b**) (Table 2 vs 3). Table 3 summarizes selected properties of **1b**−**3b**, together with those of related complexes in the literature. The λ_{max} values

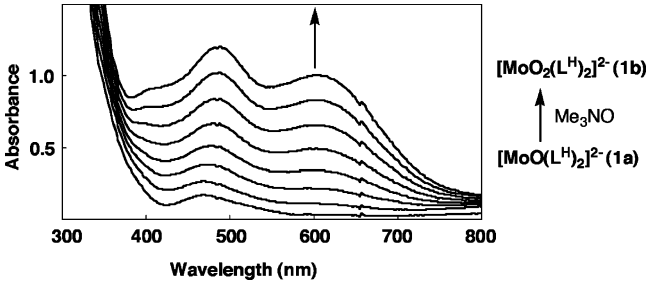

Figure 4. Spectral changes during the reaction of $[Mo^{IV}O(L^H)_2]^{2-}$ (**1a**) to $[Mo^{VI}O_2(L^H)_2]^{2-}$ (**1b**) by treatment with Me_3NO in CH_3CN: $[Mo^{IV}O(L^H)_2{}^{2-}]$ = 0.3 mM, $[Me_3NO]^0$ = 15 mM.

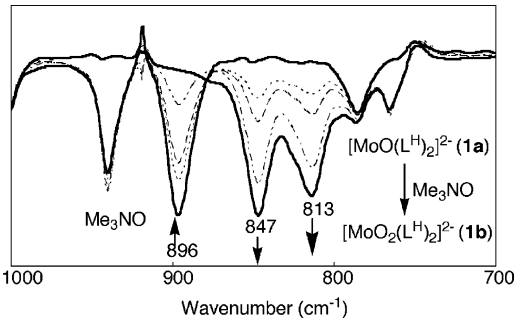

Figure 5. Time-dependent IR spectral changes during the reaction of $[MoO(L^H)_2]^{2-}$ (**1a**, 15 mM) with Me_3NO (75 mM) in CH_3CN to produce $[MoO_2(L^H)_2]^{2-}$ (**1b**). The spectra were recorded at 0, 3, 5, 10, and 15 min after the treatment, respectively.

(23) Donahue, J. P.; Goldsmith, C. R.; Nadiminti, U.; Holm, R. H. *J. Am. Chem. Soc.* **1998**, *120*, 12869.
(24) Lim, B. S.; Holm, R. H. *J. Am. Chem. Soc.* **2001**, *123*, 1920.
(25) Because the observed m/z = 418 value corresponded to its mono anionic state, one-electron oxidation of the formed $[Mo^{VI}O_2(L^H)_2]^{2-}$ was suggested to take place during the measurement.
(26) Topich, J.; Bachert, J. O. *Inorg. Chem.* **1992**, *31*, 511.

Table 3. Selected Properties of $Mo^{VI}O_2$ Complexes and Arsenite Oxidase

	λ_{max} (nm)	ν(Mo=O) (cm^{-1})	E_{pa} (V vs SCE)	ref
arsenite oxidase	470, 670	(822)[a]	*b*	26
$(Et_4N)_2[MoO_2(L^H)_2]$ (**1b**)	490, 606	847, 813	−0.36	*c*
$(Et_4N)_2[MoO_2(L^S)_2]$ (**2b**)	474, 592	850, 818	−0.27	*c*
$(Et_4N)_2[MoO_2(L^O)_2]$ (**3b**)	490, 594	855 (853)[a], 820	−0.23	*c*
$(Et_4N)_2[MoO_2(bdt)_2]$	430, 540	858 (858)[a], 831	+0.07	11
$(Bu_4N)_2[MoO_2(mnt)_2]$	390, 430	885 (885)[a], 852	*b*	10a 11
$[MoO_2(Et_2NCS_2)_2]$	380	905, 877	*b*	7
$[MoO_2(Sphe)_2]$[d]	412	912, 880	*b*	8
$[MoO_2(dmp)]$[e]	385, 449	950, 915	*b*	9

[a] Number in parenthesis is the Raman shift. [b] Not observed. [c] This work. [d] Sphe = *N*,*N*′-dimethyl-*N*,*N*′-bis(2-mercaptophenyl)ethylenediamine. [e] dmp = 2,6-bis(2,2-diphenyl-2-mercaptoethanyl)pyridine.

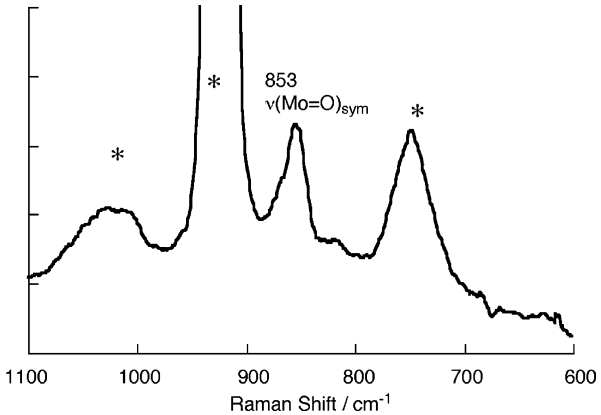

Figure 6. Resonance Raman spectrum of $[MoO_2(L^O)_2]^{2-}$ (**3b**) in CH_3CN.

of the UV−vis spectra of **1b**−**3b** were larger than those of the reported $Mo^{VI}O_2$ complexes with the bdt,[11] mnt,[10a] Et_2NCS_2, Sphe, and dmp ligands.[7−9] Thus, the energy levels of the filled orbitals of the S atoms in the L^H, L^S, and L^O ligands are enough high to offer strong interactions between the dithiolene S(pπ) orbitals and Mo(dπ) orbitals and to increase the covalent character of the Mo−S bonds. Interestingly, complexes **1b**−**3b** have UV−vis peak shapes and positions similar to those of the oxidized state of arsenite oxidase (470 and 670 nm),[27] suggesting that the absorption bands observed with arsenite oxidase may have charge-transfer characteristics from the dithiolene to the six-coordinated *cis*-MoO_2 core. Complexes **1b**−**3b** have lower frequency Mo=O stretching bands than those of $(Et_4N)_2[MoO_2(bdt)_2]$ (858 and 831 cm^{-1}),[11] $(Bu_4N)_2[MoO_2(mnt)_2]$ (885 and 852 cm^{-1}),[10a] and $[MoO_2(Et_2NCS_2)_2]$ (905 and 877 cm^{-1}),[7] indicating that they have relatively weak Mo^{VI}=O bonds. Probably, the O → Mo electron donation decreased to weaken the Mo=O bonds as the S → Mo electron donation increased. In addition to the strong interactions between the dithiolene S orbitals and the Mo orbitals, the aliphatic dithiolenes employed may provide strong trans influences compared with those of the ligands in $(Et_4N)_2[MoO_2(bdt)_2]$, $(Bu_4N)_2[MoO_2(mnt)_2]$, and $[MoO_2(Et_2NCS_2)_2]$. Figure 6 illustrates a resonance Raman spectrum of **3b**. A strong Raman band was observed at 853 cm^{-1}.[28] Because strong Raman bands around 900 cm^{-1} have been assigned to a $\nu(Mo=O)_{symm}$ stretching band in other $Mo^{VI}O_2$ bis(dithiolene) complexes,[29] the IR band observed at high wavenumbers (855 cm^{-1}) in **3b** was also assigned to a $\nu(Mo=O)_{symm}$ stretch. The $\nu(Mo=O)_{symm}$ stretching bands (847 cm^{-1} for **1b**, 850 cm^{-1} for **2b**, and 855 cm^{-1} for **3b**)[30] were close to that of arsenite oxidase (822 cm^{-1}),[5] although the bands of other $Mo^{VI}O_2$ complexes are reported at higher wavenumbers: mnt, 885 cm^{-1};[10a] bdt, 858 cm^{-1};[11] Et_2NCS_2, 905 cm^{-1};[7] L1, 912 cm^{-1};[8] and L2, 950 cm^{-1}.[9] The fact that the value for **1b** (847 cm^{-1}) was higher than that of the oxidized state of arsenite oxidase (822 cm^{-1}) suggests a possibility that the oxo groups of the arsenite oxidase interact with the peptide backbone through hydrogen bonds. Similar effects of hydrogen bonding were reported in some synthetic complexes: $(Ph_4P)_2[MoO(sdt)_2]\cdot C_2H_5OH$, in which the oxo group interacted with ethanol, exhibited a ν(Mo=O) stretching band at 879 cm^{-1}, while the $(Ph_4P)_2[MoO(2\text{-pedt})_2]$ (2-pedt = 1-(2-pyridine)-1,2-ene-dithiolate) and $(Ph_4P)_2[MoO(4\text{-pedt})_2]$ (4-pedt = 1-(4-pyridine)-1,2-ene-dithiolate) complexes had bands at 902 and 900 cm^{-1}, respectively.[16]

The redox potential values of **1b**−**3b** were more negative than that of $(Et_4N)_2[MoO_2(bdt)_2]$ (+0.07 V).[11] These results may correlate with the strengths of the Mo=O bonds, and probably indicate that, as the electron-donating property of the ligands increases, the O → Mo electron donation decreases, leading to the weakened Mo=O bond character of **1b**−**3b**. The redox potentials shifted to more negative values in the order L^H (−0.36 V) < L^S (−0.27 V) < L^O (−0.23 V), which parallels that of the Mo=O stretching bands observed at low energies (L^H (847 cm^{-1}) < L^S (850 cm^{-1}) < L^O (855 cm^{-1})).[31] The natures of the substituents on the dithiolene ligands employed here obviously altered the Mo=O bond characters in the $Mo^{IV}O$ and $Mo^{VI}O_2$ complexes.

Complexes **1b**−**3b** showed markedly different reactivities from those of $[MoO_2(mnt)_2]^{2-}$. The monitoring of the characteristic absorption bands at 400−700 nm demonstrated that they did not react with excess PPh_3 in CH_3CN but, rather, decomposed with the addition of H_2O and CH_3OH. Because the $[MoO_2(mnt)_2]^{2-}$ complex reacted with PPh_3 and was stable in a CH_3CN/H_2O solution,[10] the weakened Mo=O bond characters of **1b**−**3b** enhanced the basicity of the oxygen atoms in the $Mo^{VI}O_2$ cores to provide unique reactivities.

We have demonstrated that a new series of $Mo^{VI}O_2$ complexes containing aliphatic dithiolene ligands L^H, L^S, and L^O were readily prepared by the oxidation of their $Mo^{IV}O$ precursors. The characteristics of the Mo=O bonds in the $Mo^{IV}O$ and $Mo^{VI}O_2$ states could be changed significantly by

(27) Anderson, G. L.; Williams, J.; Hille, R. *J. Biol. Chem.* **1992**, *267*, 23674.
(28) We did not succeed in taking resonance Raman spectra of **1b** and **2b**, suggesting that the Mo=O bonds might have photolabile natures.
(29) Johnson, M. K. In *Progress in Inorganic Chemistry*; Karlin, K. D., Stiefel, E. I., Eds.; John Wiley & Sons: New York, 2004; Vol. 52, p 213.
(30) Because the intensities and values of the IR bands at high wavenumber of **1b** and **2b** were similar to those of **3b**, they were also assigned to $\nu(Mo=O)_{symm}$ stretching bands.
(31) The order could not be interpreted by considering the partial charges on the sulfur atoms in the free dithiolato forms ($[L^H]^{2-}$, $[L^S]^{2-}$, and $[L^O]^{2-}$). All of the partial charges on the sulfur atoms were calculated to be −0.77 by the CONFLEX Japan/MM3 program, while the charges on the sulfur atoms of bdt^{2-} were calculated to be −0.73.

substitution on the dithiolene ligands. Because the Mo═O bond characteristics in these complexes can be finely tuned, the type of aliphatic ligands employed here could be very useful for modeling molybdenum cofactor families.

Acknowledgment. The authors are grateful to Professor Norikazu Ueyama of Osaka University for valuable comments. This work was partly supported by grants for Scientific Research (No. 16750052 to H.S.) from the Japan Society for Promotion of Science and for CREST of the Japan Science and Technology Agency (JST).

Supporting Information Available: ORTEP drawings of $(Et_4N)_2[MoO(L^S)_2]$ (**2a**) and $(Et_4N)_2[MoO(L^O)_2]$ (**3a**) (Figure S1), cyclic voltammograms of the $[MoO(L)_2]^{2-}/[MoO_2(L)_2]^{2-}$ complexes (**1a**−**3a** and **1b**−**3b**) (Figure S2), ESI-MS of $[MoO_2(L)_2]^{2-}$ (**1b**−**3b**) (Figure S3), electronic spectral changes of $[MoO(L)_2]^{2-}/[MoO_2(L)_2]^{2-}$ (**2a**, **3a**/**2b**, **3b**) (Figure S4), and IR spectral changes of $[MoO(L)_2]^{2-}/[MoO_2(L)_2]^{2-}$ (**2a**, **3a**/**2b**, **3b**) (Figure S5). This material is available free of charge via the Internet at http://pubs.acs.org.

IC050234P